JOURNAL OF VIROLOGY, July 2009, p. 6978–6986 Vol. 83, No. 14
0022-538X/09/$08.00+0 doi:10.1128/JVI.00598-09

Comparison of the Pseudorabies Virus Us9 Protein with Homologs from Other Veterinary and Human Alphaherpesviruses[▽]

M. G. Lyman, C. D. Kemp,† M. P. Taylor, and L. W. Enquist*

Department of Molecular Biology, Princeton University, Princeton, New Jersey 08544

Received 23 March 2009/Accepted 24 April 2009

Pseudorabies virus (PRV) Us9 is a small, tail-anchored (TA) membrane protein that is essential for axonal sorting of viral structural proteins and is highly conserved among other members of the alphaherpesvirus subfamily. We cloned the Us9 homologs from two human pathogens, varicella-zoster virus (VZV) and herpes simplex virus type 1 (HSV-1), as well as two veterinary pathogens, equine herpesvirus type 1 (EHV-1) and bovine herpesvirus type 1 (BHV-1), and fused them to enhanced green fluorescent protein to examine their subcellular localization and membrane topology. Akin to PRV Us9, all of the Us9 homologs localized to the *trans*-Golgi network and had a type II membrane topology (typical of TA proteins). Furthermore, we examined whether any of the Us9 homologs could compensate for the loss of PRV Us9 in anterograde, neuron-to-cell spread of infection in a compartmented chamber system. EHV-1 and BHV-1 Us9 were able to fully compensate for the loss of PRV Us9, whereas VZV and HSV-1 Us9 proteins were unable to functionally replace PRV Us9 when they were expressed in a PRV background.

Alphaherpesviruses are classified by their variable host range, short reproductive cycle, and ability to establish latency in the peripheral nervous system (PNS) (36, 37). Commonly studied pathogens of this subfamily include herpes simplex virus (HSV) and varicella-zoster virus (VZV), as well as the veterinary pathogens pseudorabies virus (PRV), equine herpesvirus (EHV), and bovine herpesvirus (BHV). Initial infection begins with the virus entering the host mucosal surfaces and spreading between cells of the mucosal epithelium. Invariably, virus enters the PNS through the infection of peripheral nerves that innervate this region. The virus establishes a latent infection in PNS neurons that can be reactivated and that persists for the life of the host (36). In most natural infections, virus replication in the PNS never spreads to the central nervous system (CNS). However, on rare occasions, invasion of the CNS does occur, resulting in devastating encephalitis (46). Trafficking of virus particles from infected epithelial cells into the axon and subsequent transport to neuronal cell bodies is known as retrograde spread of infection. Trafficking of virus particles that are assembled in the neuronal cell body and subsequently sorted into axons for transport to epithelial cells at the initial site of infection (upon reactivation from latency) is known as anterograde spread of infection.

Though the natural host of PRV is swine, the virus infects a wide variety of animals, including rodents, cats, dogs, rabbits, cattle, and chicken embryos, but not higher primates (1, 30, 47). In contrast to the well-contained spread of PRV within its natural host, infection of other mammals is usually lethal. Instead of stopping in the PNS, infection continues on to second-order and third-order neurons in the CNS (reviewed in reference 35). This facet of PRV infection makes it a useful tracer of neuronal connections (18). Work in our lab has identified three PRV proteins, Us9 and the gE/gI heterodimer, which are critical for efficient anterograde spread of infection in vivo (i.e., spread from presynaptic to postsynaptic neurons) (6, 45). The molecular mechanism by which these proteins function has been further elucidated in vitro using primary neuronal cultures of superior cervical ganglion (SCG) harvested from embryonic rat pups. PRV Us9 and, to a lesser extent, gE/gI are required for efficient axonal targeting of viral structural proteins, a necessary step for subsequent anterograde, transneuronal spread (10, 11, 27, 28, 42).

PRV Us9 is a type II, tail-anchored (TA) membrane protein that is highly enriched in lipid raft microdomains and resides predominantly in or near the *trans*-Golgi network (TGN) inside infected cells (5–7, 27). It has homologs in most of the alphaherpesviruses, including VZV (16), HSV-1 (22), HSV-2 (17), EHV-1 (21, 40), EHV-4 (41), BHV-1 (25), and BHV-5 (14). Though several studies have examined individually the Us9 proteins encoded by VZV (16), HSV-1 (4, 22, 34, 39), BHV-1 (13), and BHV-5 (14), several gaps in our understanding of Us9 biology remain, namely, whether all of the PRV Us9 homologs are type II membrane proteins, if the proteins localize to similar subcellular compartments within different cell types, and if they can functionally substitute for the loss of PRV Us9 in axonal sorting and anterograde spread of infection. The aim of this study is to examine PRV Us9 in parallel assays with its homologs from VZV, HSV-1, EHV-1, and BHV-1 to identify potential similarities and differences between these highly conserved alphaherpesvirus proteins.

MATERIALS AND METHODS

Culturing of PK15 cells. Porcine kidney (PK15) epithelial cells were maintained at 37°C in Dulbecco's modified Eagle medium supplemented with 10% fetal bovine serum and Pen/Strep (HyClone) in a 5% CO_2 environment.

Plasmids. pEGFP-N1 (where EGFP is enhanced green fluorescent protein) was purchased from Clontech (Palo Alto, CA). The construction of pBB14 has been reported previously (5), and the plasmid contains the Us9 gene from the wild-type laboratory strain PRV Becker cloned into EGFP-N1, resulting in the fusion of EGFP to the C terminus of PRV Us9. GalT-mRFP1(where GalT is

* Corresponding author. Mailing address: 314 Schultz Laboratory, Department of Molecular Biology, Princeton, NJ 08544. Phone: (609) 258-2415. Fax: (609) 258-1035. E-mail: lenquist@princeton.edu.

† Present address: Department of Surgery, The Johns Hopkins Hospital, Baltimore, MD 21287.

▽ Published ahead of print on 6 May 2009.

TABLE 1. Template and primer pairs for the amplification of VZV, HSV-1, EHV-1, and BHV-1 Us9 homologs for subsequent cloning into pEGFP-N1

Plasmid	Template	Us9 primer[a]	
		Direction	Sequence (5′ to 3′)
pHA1	HindIII C fragment of the VZV Us region	FOR	CCGGAATTCTGGATTTCT**ATG**GCCG
		REV	GCCCGGGATCCGCTCAACAAATTGTGACG
pCK113	HSV-1 strain 17 nucleocapsid DNA	FOR	TGAATTCCGCCCGCATTCCGAC**ATG**ACGTCCCGGCTC
		REV	TTGGATCCCGGCGGAGCAGCCACAT
pCK114	EcoRI/BamHI fragment of the PvuII B fragment of EHV-1 KyA strain	FOR	TGAATTCCGCCCGCATTCCGAC**ATG**GAGAAGGCGGAGG
		REV	TTGGATCCCGCGGAAACACGCGTGCCAAGAACG
pCK115	HindIII F fragment of the BHV-1 Jura strain DNA	FOR	TGAATTCCGCCCGCATTCCGAC**ATG**GAGAGTCCACG CAGC
		REV	TTGGATCCCGGGGCCGGGGCCGGGGCACTACC

[a] FOR, forward, with EcoRI site underlined and start methionine in bold; REV, reverse, with BamHI site underlined.

β-1,4-galactosyltransferase and mRFP1 is a monomeric red fluorescent protein) (23), a marker of the TGN, was a kind gift from Jennifer Lippincott-Schwartz (NIH). Plasmids containing the HindIII C fragment of the VZV unique short (Us) region, the EcoRI/BamHI fragment of the PvuII B fragment of the EHV-1 KyA strain, and the HindIII F fragment of the BHV-1 Jura strain were kindly provided by Chuck Grose (University of Iowa), D. J. O'Callaghan (Louisiana State University), and S. I. Chowdhury (Louisiana State University), respectively.

Antibodies. Antibodies used in this report include the following: rabbit polyclonal antiserum recognizing PRV Us9 (5), goat polyclonal antiserum recognizing PRV Us2 (15), rabbit polyclonal antiserum recognizing VZV Us9 (16) (a kind gift from Jeffrey Cohen, NIH), rabbit polyclonal antiserum recognizing HSV-1 Us9 (a kind gift from Harvey Friedman, University of Pennsylvania), and goat polyclonal antiserum recognizing BHV-1 Us9 (13) (a kind gift from Shafiqul I. Chowdhury, Louisiana State University). Rabbit polyclonal anti-GFP antibody was purchased from Clontech. The Alexa Fluor 546 secondary antibody (used at 1:500) was purchased from Molecular Probes.

Cloning of VZV, HSV-1, EHV-1, and BHV-1 Us9 ORFs and subsequent fusion to EGFP. Us9 open reading frames (ORFs) were amplified with *Pfu* DNA polymerase (Stratagene, La Jolla, CA) using the templates and primers described in Table 1. Forward primers contained an EcoRI linker, and reverse primer contained a BamHI linker that also converted the Us9 stop codon to an arginine codon (alanine codon for VZV Us9). PCR conditions were as follows: one cycle of 96° for 5 min; 2 cycles of 96° for 1 min, 55° for 30 s, and 72° for 45 s; and 25 cycles of 96° for 1 min, 62° for 45 s, and 72° for 45 s, followed by one cycle of 72° for 4 min. The resulting PCR products were purified and digested with EcoRI and BamHI. The digested DNA was subsequently ligated into pEGFP-N1 (also digested with EcoRI and BamHI), resulting in the fusion of EGFP to the C terminus of the Us9 ORFs (under the control of the cytomegalovirus [CMV] immediate-early promoter). The resulting plasmids (pHA1, VZV Us9-EGFP; pCK113, HSV-1 Us9-EGFP; pCK114, EHV-1 Us9-EGFP; and pCK115, BHV-1 Us9-EGFP) were transformed via electroporation into DH5-α *Escherichia coli* cells and confirmed by restriction digest and sequencing to ensure that no mutations were introduced during PCR amplification.

Transfection and imaging of PK15 cells. PK15 cells were grown on glass coverslips (~20% confluence) and cotransfected with GalT-mRFP1 and PRV Us9-EGFP (pBB14), VZV Us9-EGFP (pHA1), HSV-1 Us9-EGFP (pCK113), EHV-1 Us9-EGFP (pCK114), or BHV-1 Us9-EGFP (pCK115). Lipofectamine 2000 was used for transfection as directed by the manufacturer's instructions (Invitrogen, Carlsbad, CA). At 30 h posttransfection, cells were washed with phosphate-buffered saline (PBS) and fixed with 4% paraformaldehyde in PBS for 10 min. After fixation, cells were washed three times with PBS, mounted on a glass slide using Aqua-Poly/Mount (Polysciences, Warrington, PA), and allowed to air dry for 24 h prior to imaging. Direct fluorescence was visualized on a Leica SP5 confocal microscope using appropriate excitation and emission filters.

Membrane topology of PRV Us9 and its homologs. Transfection of pEGFP-N1, pBB14, pHA1, pCK113, pCK114, and pCK115 into PK15 cells was performed as described above. At 30 h posttransfection, cells were washed three times with PBS and fixed with 4% paraformaldehyde in PBS for 10 min. Cells were then washed three times with PBS and labeled with GFP polyclonal antiserum (1:200 dilution; Clontech) in nonpermeabilizing buffer (3% bovine serum albumin [BSA] in PBS) for 30 min. For the "permeabilized" cell control, 0.5% saponin was added to the 3% BSA–PBS mixture. After cells were labeled with primary GFP antibody, they were washed three times with PBS, and Alexa Fluor 546-conjugated secondary antiserum (1:500 in nonpermeabilizing wash buffer; Molecular Probes, Eugene, OR) was placed on cells for an additional 30 min. Cells were washed three times with PBS and mounted on a glass slide using Aqua-Poly/Mount (Polysciences, Warrington, PA) and allowed to air dry for 24 h prior to imaging. Fluorescence was visualized on a Nikon MRC600 confocal microscope using appropriate excitation and emission filters.

Construction of PRV strains expressing VZV, HSV-1, EHV-1, and BHV-1 Us9 homologs. PRV 164 has a deletion of the endogenous Us9 ORF and contains a CMV-driven PRV Us9-EGFP expression cassette inserted into the gG locus (26). This was the parental virus used to construct PRV 328, PRV 334, PRV 335, PRV 336, and PRV 337. The construction of PRV 328 was briefly described previously (26); this virus strain expresses wild-type PRV Us9 under the CMV promoter in the gG locus. A QuikChange II site-directed mutagenesis kit (Stratagene, La Jolla, CA) was used to introduce a stop codon between the PRV Us9 and EGFP ORFs of pBB14 (becoming pML101). Approximately 3 to 4 μg of pML101 was digested with NsiI, heat inactivated for 20 min at 80°C, and transfected into PK15 cells (~10^7 cells) with 2 μg of PRV 164 genomic DNA using Lipofectamine 2000 following the manufacturer's instructions (Invitrogen, Carlsbad, CA). Targeted homologous recombination between pML101 (CMV-PRV Us9-stop-EGFP) and the CMV-Us9-EGFP expression cassette in the gG locus of PRV 164 was predicted to occur between the 5′ homologous arm of the NsiI fragment containing the CMV promoter and the 3′ homologous arm containing the EGFP ORF and simian virus 40 poly(A) sequence. When full cytopathic effect was observed, usually between 48 to 72 h, the cells and medium were collected together and serially diluted for the isolation of individual plaques. Plaques not expressing EGFP were identified using a Nikon Eclipse TE300 inverted epifluorescence microscope and then subjected to three rounds of plaque purification. Expression of PRV Us9 under the CMV promoter in the gG locus was confirmed by Western blot analysis (the strain was designated PRV 328). The construction and isolation of PRV Us9-null strains expressing VZV Us9 (PRV 334), HSV-1 Us9 (PRV 335), EHV-1 Us9 (PRV 336), and BHV-1 Us9 (PRV 337) were constructed in a similar manner to PRV 328. Stop codons were introduced by site-directed mutagenesis between the Us9 ORFs and the EGFP ORF of the mammalian expression constructs pHA1 (VZV Us9-EGFP), pCK113 (HSV-1 Us9-EGFP), pCK114 (EHV-1 Us9-EGFP), and pCK115 (BHV-1 Us9-EGFP). With the introduction of stop codons, these plasmids became pML112 (VZV Us9), pML113 (HSV-1 Us9), pML114 (EHV-1 Us9), and pML115 (BHV-1 Us9). Subsequent steps for the construction of these PRV strains were identical to those followed for PRV 328 (i.e., plasmid DNA was digested with NsiI, heat inactivated, transfected with PRV 164 DNA in PK15 cells, which were allowed to undergo full cytopathic effect, and nongreen plaques were purified, etc.). Expression of VZV, HSV-1, and BHV-1 Us9 proteins was confirmed by Western blot analysis. Transcription of the mRNA containing the EHV-1 Us9 ORF was confirmed by reverse transcription-PCR (RT-PCR) analysis. Total RNA from infected PK15 cells (~3×10^6) was isolated at 6 h postinfection (hpi) using an RNeasy minikit following the manufacturer's instructions (Qiagen). Primer sets that amplified 500-bp fragments of the EHV-1 Us9 and EGFP ORFs (the pair EHVUs9 F,5′-ATGGAGAAGGCGGAGGC-3′, and EHVUs9R, 5′-TTCATTGTCGCTCTCGC-3′; and the pair EGFPF,5′-ATGGTGAGCAAGGGCGAG-3′, and EGFPR, 5′-GATCTTGAAGTTCACCTTG-3′) were added to purified RNA and components of the OneStep RT-PCR kit (Qiagen) as recommended.

Western blot analysis. To analyze steady-state viral protein expression, PK15 cells (~3.0×10^6) were infected at a high multiplicity of infection (MOI) with PRV 328, PRV 334, PRV 335, PRV 336, or PRV 337. At 6 hpi, medium was

removed, and infected cells were scraped into 330 μl of PBS and 170 μl of 3× Laemmli sample buffer. Samples were homogenized with an insulin syringe, boiled for 2 min, and subjected to sodium dodecyl sulfate-polyacrylamide gel electrophoresis. All gels were transferred to an Immobilon-P membrane using a semidry transfer apparatus following the manufacturer's instructions (Labconco, Kansas City, MO). Following transfer, membranes were immediately put into blocking solution (2% BSA in TBS [50 mM Tris, 200 mM NaCl, 0.1% Tween-20 (vol/vol)]) and incubated for 15 min at room temperature. Primary antibody was diluted in 2% BSA-TBS-Tween solution, and allowed to rock for 30 min with the membrane. Following the 30-min incubation, the membrane was washed three times with TBS-Tween and placed in horseradish peroxidase-conjugated secondary antibody (1:10,000; KPL, Gaithersburg, MD) diluted in 2% BSA-TBS-Tween for 30 min. The membrane was then washed as previously described, and proteins were visualized with an ECL Plus Western blotting detection system (GE Healthcare).

Neuronal cultures. Detailed protocols for dissecting and culturing PNS neurons from rat embryos have been published previously (9). Briefly, sympathetic neurons from the SCGs were dissected from rat embryos at embryonic day 15.5 to 16.5 (Sprague-Dawley rats; Hilltop Labs, Inc., Scottdale, PA) and incubated in 250 μg/ml of trypsin (Worthington Biochemicals) for 15 min. Trypsin inhibitor (1 mg/ml; Sigma Aldrich) was added to neutralize the trypsin for 5 min and then removed and replaced with neuron culture medium (described below). Prior to plating, the ganglia were triturated using a fire-polished Pasteur pipette. The neuron culture medium consists of Neurobasal medium (without L-glutamine) (Invitrogen), penicillin-streptomycin-glutamine (Invitrogen), B-27 serum-free supplement (Invitrogen), and 100 ng/ml of nerve growth factor 2.5S (Invitrogen). Two days after plating, the neuronal cultures were treated with a 1 μM concentration of the antimitotic drug cytosine ß-D-arabinofuranoside (Sigma Aldrich) to eliminate any nonneuronal cells. The neuron culture medium was replaced every 3 to 4 days, and cultures were maintained in a humidified, CO_2-regulated, 37°C incubator. All experimental protocols related to animal use were approved by the Institutional Animal Care and Use Committee of the Princeton University Research Board under protocol number 1691 and are in accordance with the regulations of the American Association for Accreditation of Laboratory Animal Care and those in the Animal Welfare Act (Public Law 99-198).

Trichamber culture system. Protocols for assembling the trichamber system have been described previously (11, 12). Tools and reagents, including the Teflon rings (Tyler Research, Alberta, Canada) and the silicone grease-loaded syringe (Dow Corning), were sterilized by autoclaving prior to assembly. Tissue culture dishes (35 mm) were coated with 500 μg/ml of poly-DL-ornithine (Sigma Aldrich) in borate buffer, followed by 10 μg/ml of natural mouse laminin (Invitrogen), and then washed and dried; the bottom surface of each dish was etched with a pin rake, creating a series of 20 evenly spaced grooves. We used a silicone grease-loaded syringe attached to an 18-gauge truncated hypodermic needle to apply a thin, continuous strip of silicone grease over the entire bottom surface of the Teflon ring. Next, a 50-μl drop of 1% methocellulose and 1× Dulbecco's modified Eagle medium (serum free) was placed in the center of each tissue culture dish covering the etched grooves. This step prevents the seal from being entirely devoid of moisture, which is needed for axon penetration and growth between the grooves. Finally, the silicone grease-coated ring was gently seated on the tissue culture dish or the surface of the 35-mm dish such that the etched grooves spanned all three compartments, forming a watertight seal between compartments. Neuron medium was then placed in all three compartments immediately after the chamber was assembled. Once the SCG neurons were dissected and dissociated, approximately two-thirds of a single ganglion was plated into the soma chamber (compartment S) and allowed to mature for 2 weeks in the presence of nerve growth factor. During this differentiation period, axons were guided between a series of grooves across the methocellulose compartment (compartment M) to the neurite compartment (compartment N). PK15 "indicator" cells were then plated on the neurites in compartment N 24 h prior to infection with PRV. Approximately 30 min before the addition of virus, medium in compartment M was replaced with a mix of 1% methocellulose and complete neuronal growth medium.

RESULTS

A comparison of the primary amino acid sequences between PRV Us9 and its homologs in VZV, HSV-1, EHV-1, and BHV-1 showed several conserved motifs and domains (Fig. 1). All of the Us9 proteins contain a dileucine or tyrosine-based endocytic motif. Mutation of the dileucine motif in PRV Us9 had a modest impact on the ability of Us9 to be endocytosed from the plasma membrane of swine epithelial cells (7) but did not have a noticeable role in PRV Us9-mediated anterograde transneuronal spread in vivo (8). By contrast, mutation of two tyrosines and two serines within the acidic domain region of PRV Us9 had a dramatic impact on Us9 endocytosis from the surface of infected PK15 cells, anterograde transneuronal spread of infection in the rat brain, and axonal sorting in dissociated primary neuronal cultures (8, 42). Specifically, changing the two conserved tyrosines to alanines abrogates anterograde sorting of PRV structural proteins; mutation of the two serine residues, which comprise casein kinase II phosphorylation sites, affects the rate of axonal sorting and subsequent transneuronal spread (8, 42). As shown in Fig. 1, these tyrosine and serine residues are highly conserved among all Us9 homologs.

Other prominent domains within PRV Us9 are a positively charged region, enriched in arginine residues, found immediately before a long hydrophobic stretch of amino acids that constitutes a transmembrane domain. Kyte-Doolittle hydropathy analysis of this region (Fig. 1) shows the disparate charge distribution between these domains; values greater than zero represent amino acids that are hydrophilic while negative values are hydrophobic. It is known that positively charged/basic amino acid regions located before the transmembrane domain of integral membrane proteins establish protein topology in the lipid bilayer (often referred to as the "positive-inside" rule, i.e., transmembrane proteins are orientated in such a way that positively charged arginine and lysine residues directly preceding the transmembrane domain are located within the cytoplasm) (31, 33, 43). Furthermore, in the case of TA type II membrane proteins, basic regions before or after the transmembrane domain can also impact whether the protein is posttranslationally inserted into the mitochondrial outer membrane or the endoplasmic reticulum (ER) (3). Therefore, all of the Us9 proteins shown in Fig. 1 are predicted to have a type II membrane topology, i.e., to be TA membrane proteins. Indeed, it has been shown previously that PRV Us9 and VZV Us9 are TA membrane proteins (5, 16).

To facilitate the comparison of PRV Us9 to its homologs, the Us9 ORFs of VZV, HSV-1, BHV-1, and EHV-1 were PCR amplified and cloned in-frame with EGFP (primers and PCR templates are given in Table 1). The resulting plasmids, pHA1 (VZV Us9-EGFP), pCK113 (HSV-1 Us9-EGFP), pCK114 (EHV-1 Us9-EGFP), and pCK115 (BHV-1 Us9-EGFP), were subsequently transfected into PK15 cells to analyze their subcellular localization.

PRV and VZV Us9 localize predominantly to the Golgi complex during infection (7, 16). PRV Us9-EGFP is also targeted to the TGN in transfected cells, similar to its localization inside infected cells (7). To compare the TGN localization of PRV Us9-EGFP to the that of the other Us9 homologs, we cotransfected PRV, VZV, HSV-1, EHV-1, and BHV-1 Us9-EGFP expression constructs with GalT-mRFP1 into PK15 cells (23). GalT is a membrane-bound enzyme enriched in the *trans*-Golgi cisternae and is commonly used as a marker for the TGN (32). We found that all of the Us9-EGFP constructs compartmentalized with GalT-RFP (Fig. 2), suggesting that the TGN is the primary site for steady-state localization of HSV-1, EHV-1, and BHV-1 Us9 proteins (consistent with the known localiza-

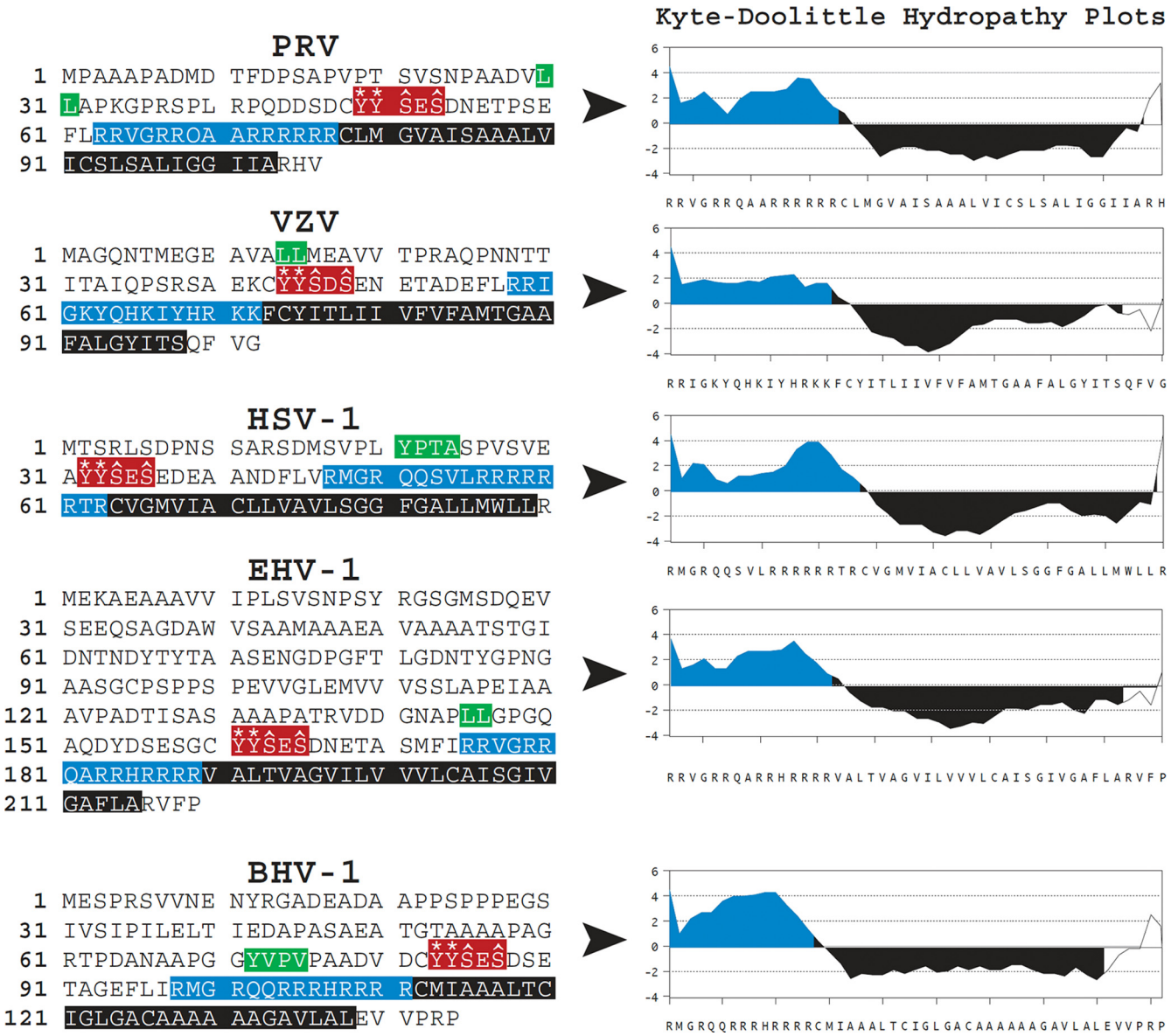

FIG. 1. Primary amino acid sequences and conserved domains of PRV, VZV, HSV-1, EHV-1, and BHV-1 Us9 proteins. The dileucine- and tyrosine-based endocytic sorting motifs are highlighted in green. A portion of the acidic cluster domains that contain key tyrosine residues (asterisks) and serine residues (carets) are highlighted in red. The basic domains, enriched in arginine and lysine residues, are highlighted in blue. The putative transmembrane domains are highlighted in black. Kyte-Doolittle hydropathy plot analyses (performed in MacVector, version 10.0) show the relative differences in hydrophilicity/hydrophobicity between the basic and transmembrane domains of the various Us9 proteins.

tion of PRV and VZV Us9). Slight plasma membrane staining was also observed in all cells expressing Us9-EGFP, consistent with the idea that a small population of Us9 cycles between the plasma membrane and the TGN (7).

Though it has been shown that PRV and VZV Us9 are type II, TA membrane proteins (with their short C termini exposed to the lumen/cell surface and their N termini in the cytosol) (5, 16), it remained unclear if HSV-1, EHV-1, and BHV-1 Us9 proteins were also type II integral membrane proteins. In fact, HSV-1 Us9 was originally described to be a tegument protein (22). As shown in Fig. 1, each of the Us9 homologs is predicted to have a transmembrane domain and to share similar topologies. Therefore, we examined whether all of the PRV Us9 homologs were in fact type II membrane proteins. PK15 cells were transiently transfected with PRV, VZV, HSV-1, EHV-1, and BHV-1 Us9-EGFP expression constructs for 30 h and fixed with paraformaldehyde. We reasoned that if the Us9-EGFP homologs had a type II orientation in the membrane, the EGFP moiety would be present on the surface of transfected cells and exposed to labeling with GFP polyclonal antiserum. Figure 3 illustrates this idea, with EGFP fused to the C terminus of Us9 and located on the extracellular side of the plasma membrane. Alternatively, if the proteins were in a type I orientation, GFP would not be exposed to the cell surface, and no staining would be observed in the absence of permeabilization. Figure 3A shows PK15 cells transfected with pEGFP-N1, fixed

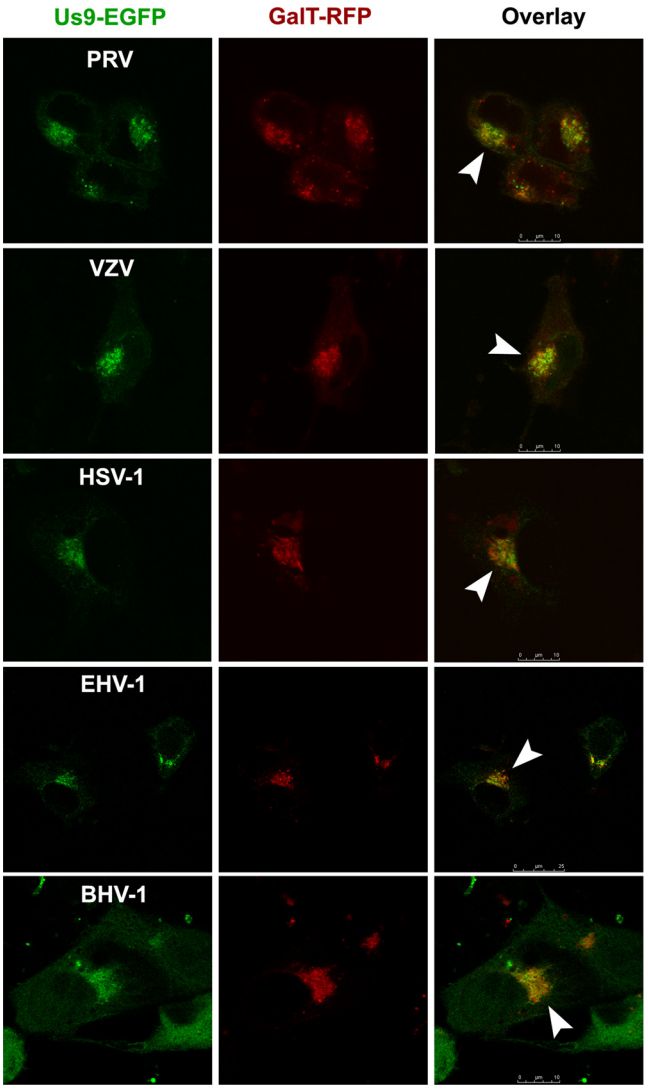

FIG. 2. PRV, VZV, HSV-1, EHV-1, and BHV-1 Us9-EGFP fusion proteins colocalize with the TGN marker GalT-RFP. Us9-EGFP and GalT-mRFP1 mammalian expression constructs were cotransfected into PK15 cells and fixed at 30 h posttransfection. Optical sections of transfected cells were acquired using a Leica SP5 confocal microscope. The overlay shows both the GFP and RFP channels. White arrowheads highlight the areas of colocalization.

with paraformaldehyde, stained with primary GFP and secondary Alexa Fluor 546 antibodies in nonpermeabilizing buffer, and imaged by confocal microscopy. Note that no "red" EGFP staining was present on the cell surface as soluble EGFP protein inside the cell is protected from anti-GFP antibody. When 0.5% saponin was added to the buffer, the plasma membrane was permeabilized, and anti-GFP antibodies were able to stain intracellular EGFP (Fig. 3B) (nuclear membrane was not solubilized). As controls for the type II topology of a membrane protein, PRV and VZV Us9-EGFPs were clearly labeled at the cell surface by GFP antiserum in nonpermeabilizing buffer (Fig. 3C and D). Us9-EGFP in the TGN remained green by direct fluorescence but was not stained by anti-GFP antibodies. All of the Us9-EGFP homologs showed similar patterns of red surface staining at the plasma membrane with internal green perinuclear staining (Fig. 3E to G). These data strongly support the notion that HSV-1, EHV-1, and BHV-1 Us9 are all type II membrane proteins (along with their previously characterized PRV and VZV Us9 counterparts).

PRV Us9 is essential for the sorting of viral structural components into the axon of infected neurons (28, 42), a process that subsequently impacts the virus's ability to undergo anterograde, transneuronal spread in vivo (6). We reasoned that since all of the Us9 homologs closely resembled PRV Us9 (i.e., were type II membrane proteins, contained critical sorting domains, and localized to the TGN), perhaps they would functionally compensate for the loss of PRV Us9 in axonal sorting and anterograde spread of infection. Thus, we constructed PRV Us9-null recombinant strains that expressed wild-type VZV, HSV-1, EHV-1, and BHV-1 Us9 proteins. These proteins were expressed ectopically as described previously for PRV 328, a virus strain that expresses wild-type PRV Us9 under the human CMV immediate-early promoter in the gG locus (26). Figure 4A contains a schematic of PRV strains expressing PRV Us9 (PRV 328), VZV Us9 (PRV 334), HSV-1 Us9 (PRV 335), EHV-1 Us9 (PRV 336), and BHV-1 Us9 (PRV 337). Western blot analysis using polyclonal antiserum against PRV Us9, VZV Us9, HSV-1 Us9, and BHV-1 Us9 confirmed the expression of these proteins from infected PK15 cell lysates collected at 6 hpi (Fig. 4B). We did not observe any cross-reactivity of the various Us9 antisera with nonconjugate Us9 homologs, consistent with the high similarity between Us9 domains and minimal primary amino acid identity (Fig. 1). Because we did not have antiserum against EHV-1 Us9, its expression was confirmed by RT-PCR on mRNA harvested from PK15 cells infected with PRV 336 (Fig. 4C). Primer sets designed to amplify 500 bp of the EHV-1 Us9 ORF and EGFP ORF were used in the RT-PCR. Note that the EHV-1 primers were able to amplify cDNA from PRV 336-infected cells but not cDNA from cells infected with PRV 328 (negative control). The EGFP ORF was detected in both samples as it is present in the Us9 mRNA transcripts but is not translated into protein due to the introduction of a stop codon between the Us9 and EGFP ORFs (see Materials and Methods).

Next, we assessed whether the Us9 homologs could functionally compensate for the loss of PRV Us9 in neuronal anterograde spread of infection. We employed a well-described, compartmentalized chamber system to assess the anterograde sorting and spread capabilities of virus strains in vitro (Fig. 5) (11, 26, 27). Briefly, dissociated SCG neurons dissected from embryonic rats are plated in compartment S and allowed to mature for 2 weeks in the presence of nerve growth factor. During this differentiation period, axons are guided between a series of grooves across the methocellulose compartment M to the neurite compartment N. PK15 indicator cells are then plated on the neurites in compartment N. Cell bodies in compartment S are infected, and virus particles sort into axons in a Us9-dependent manner (the primary infection is confined to compartment S via silicone vacuum grease and a methocellulose barrier). Thus, infectious virus particles spread into compartment N—in the anterograde direction—exclusively through axons emanating from neuronal cell bodies that contact PK15 cells.

PRV 328 (PRV Us9), PRV 161 (Us9-null), PRV 334 (VZV

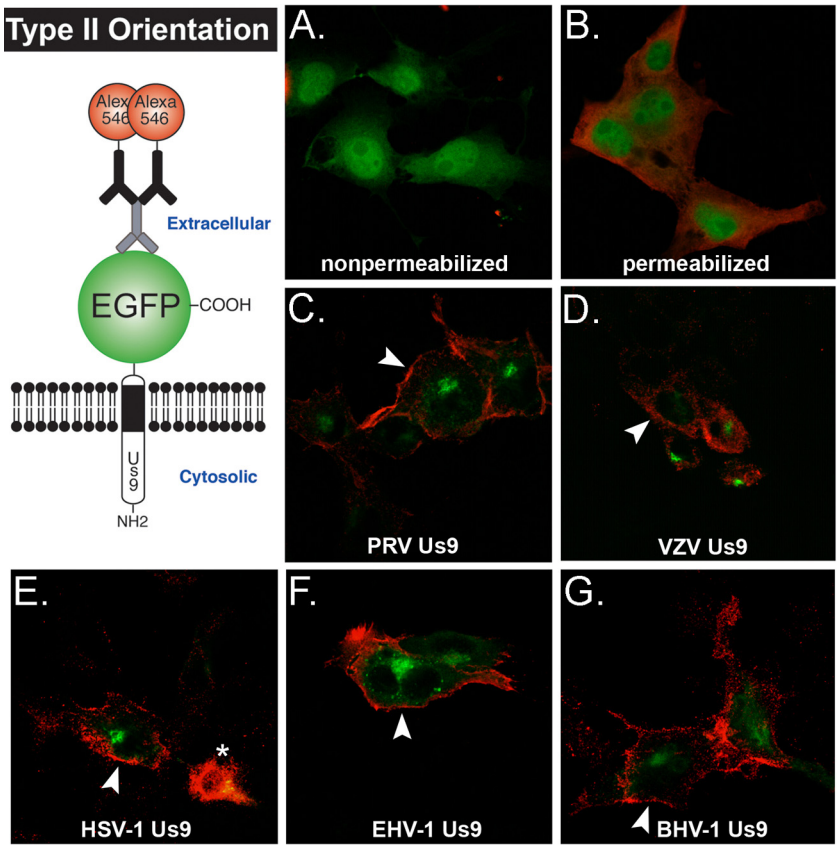

FIG. 3. PRV Us9 and its homologs have a type II membrane topology. The schematic illustrates our model for Us9-EGFP homologs with a type II orientation in the membrane. The EGFP moiety will be present on the surface of transfected cells and exposed to labeling with primary GFP polyclonal antiserum (and secondary Alexa Fluor 546-conjugated secondary antiserum) in the absence of permeabilization. PK15 cells were transiently transfected with pEGFP-N1 (A and B), pBB14 (C), pHA1 (D), pCK113 (E), pCK114 (F), and pCK115 (G); fixed at 30 h posttransfection; and labeled with GFP antiserum in nonpermeabilizing (A, C, D, E, F, and G) and permeabilizing (B) wash buffer. Optical sections of transfected cells were acquired on a Nikon MRC600 confocal microscope. White arrowheads highlight red plasma membrane staining at the cell surface. An asterisk marks dead cell debris.

Us9), PRV 335 (HSV-1 Us9), PRV 336 (EHV-1 Us9), and PRV 337 (BHV-1 Us9) were used to infect compartment S of chambers at an MOI of 10; each virus strain was examined in quadruplicate (Fig. 5). At 24 hpi, contents of both the S and N compartments were collected separately, and titers for PFU were determined on PK15 cells. PRV 328, our positive control, had a median titer of 3.7×10^5 PFU/ml in chamber S, with a median titer of 1.4×10^7 in chamber N (indicating efficient anterograde neuron-to-cell spread). PRV 161, a Us9-null mutant (6), showed a robust infection in compartment S but was essentially dead for neuron-to-cell spread of infection, with three chambers showing 0 PFU in the compartment N. One chamber had a compartment N titer of 3.7×10^3 PFU/ml. We have observed before an occasional "blip" of Us9-null mutant virus in compartment N at 24 hpi and attribute it to a single spread event (26, 27). Nevertheless, compared to PRV 328, this small amount of infectious virus is negligible. By comparison, virus strains expressing VZV Us9 and HSV-1 Us9 replicated efficiently in compartment S but showed no ability to compensate for the loss of PRV Us9 in anterograde neuron-to-cell spread; i.e., no PFU were detected in compartment N. By comparison, PRV strains expressing EHV-1 Us9 and BHV-1 Us9 were indistinguishable from PRV 328; both Us9 proteins fully complemented the loss of PRV Us9 in axonal sorting and subsequent neuron-to-cell spread.

DISCUSSION

PRV Us9 protein is a TA membrane protein that resides primarily in the TGN and is essential for sorting of virus structural proteins into the axon of infected neurons (i.e., sorting of mature virus particles within vesicles, L-particles within vesicles, or vesicles studded with viral membrane/tegument proteins) (5–8, 11, 20, 26–28, 42). In this study we examined the Us9 homologs of VZV, HSV-1, EHV-1, and BHV-1. We found that all are type II (TA) membrane proteins that localize predominantly to the TGN, indistinguishable from PRV Us9. Interestingly, the veterinary pathogens EHV-1 and BHV-1 encode Us9 proteins that are fully functional for anterograde, neuron-to-cell spread when expressed in a PRV background. By contrast, Us9 homologs from the human pathogens HSV-1 and VZV (which contain all of the conserved domains of PRV Us9) do not complement a PRV Us9-null strain.

We have demonstrated that PRV Us9 and the heterodimeric complex gE/gI play an essential role in the axonal sorting and subsequent anterograde spread of PRV in the rat nervous

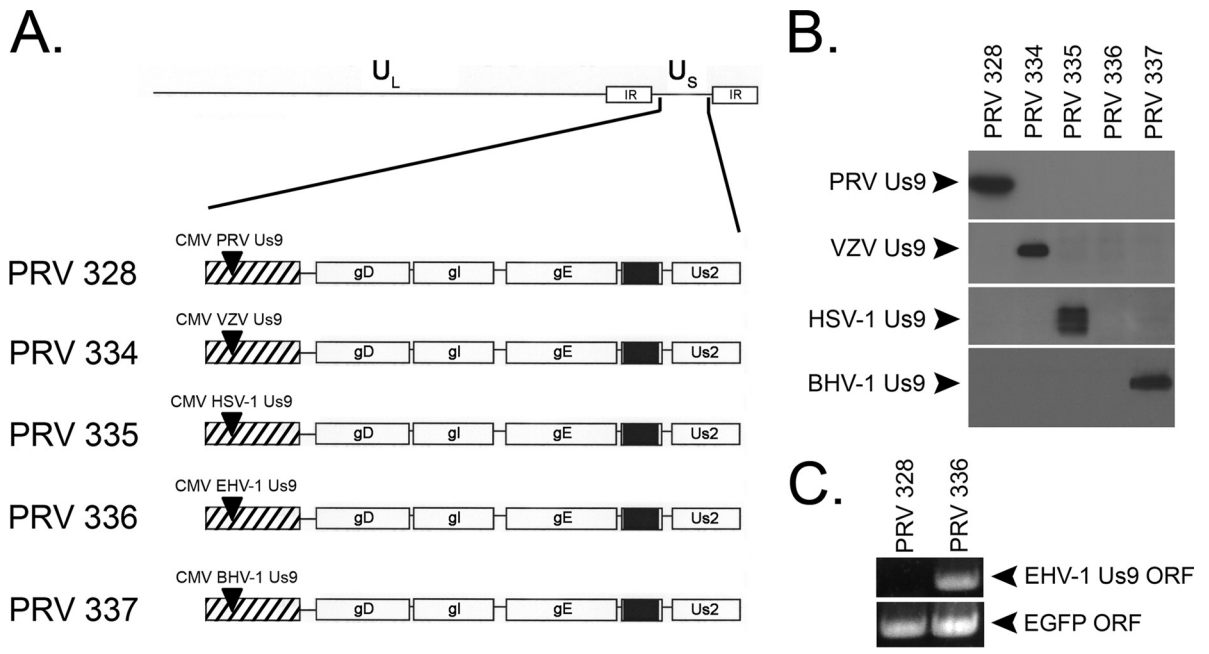

FIG. 4. Construction of PRV strains ectopically expressing Us9. (A) Schematic representation of the genomes of PRV 328 (PRV Us9), PRV 334 (VZV Us9), PRV 335 (HSV-1 Us9), PRV 336 (EHV-1 Us9), and PRV 337 (BHV-1 Us9) (adapted from Lyman et al. [26]). Note that the endogenous PRV Us9 ORF is deleted (black box between gE and Us2) and that the Us9 proteins are expressed under the CMV promoter in the nonessential gG locus (hatched box). (B) Western blot analysis on PK15 cells infected with PRV 328, PRV 334, PRV 335, PRV 336, and PRV 337. Lysates were harvested at 6 hpi. There was no cross-reactivity between the various polyclonal antisera and nonconjugate Us9 proteins (entire gels not shown). (C) As no available antiserum exists for EHV-1 Us9, we confirmed its mRNA expression via RT-PCR using primer sets specific for the EHV-1 Us9 ORF (virus expressing the PRV Us9 mRNA, PRV 328, was used as a negative control). All of the Us9-expressing strains contain the EGFP ORF in their mRNA transcripts, but it is not translated due to a stop codon inserted directly after the Us9 ORF (see Materials and Methods).

system, as well as dissociated infected SCGs harvested from embryonic rat pups (6, 10, 28, 42, 45). Though viral mutants bearing deletions of PRV Us9 or gE/gI have indistinguishable transneuronal spread phenotypes in the rat visual system (6, 45), compartmented trichamber technology enables a more sensitive evaluation of the individual impact of these proteins on axonal sorting and subsequent spread of infection (11). Ch'ng and Enquist reported that deletion of gI or gE resulted in a modest reduction in anterograde neuron-to-cell spread, with a 1- to 2-log reduction in compartment N titers, respectively. However, deletion of PRV Us9 resulted in a 4- to 5-log reduction in compartment N titers (11). Axonal sorting studies in dissociated SCG neurons with Us9- and gE-null mutants also support these trichamber findings, i.e., that deletion of PRV Us9 completely blocks the entry of viral structural proteins into the axon, whereas deletion of PRV gE results in a reduction of viral proteins in axons (a "leaky" sorting phenotype) (10, 28). Together, these data support the notion that PRV Us9 is the critical component for efficient axonal sorting of virus structural proteins though all three proteins are required to achieve maximal sorting efficiency. It is also important that PRV Us9 and gE/gI are enriched in lipid raft microdomains and that localization of Us9 to lipid rafts is critical for its function (10, 19, 27). Thus, Us9 and gE/gI may be working together, within a specialized domain of vesicular membranes, to recruit axonal sorting machinery.

Why are Us9 homologs of the human pathogens VZV and HSV-1 unable to functionally replace PRV Us9? The simplest answer may be based in alphaherpesvirus phylogeny. Phylogenetic analyses comparing the DNA and protein sequence of the viral glycoprotein gB (from 14 alphaherpesviruses) showed that PRV was more closely related to the veterinary pathogens BHV-1 and EHV-1 and more distantly related to the human pathogens VZV and HSV-1 (29). These findings correlate with the ability of BHV-1 and EHV-1 Us9 to compensate for the loss of PRV Us9 in anterograde neuron-to-cell spread (Fig. 5). However, despite these findings, VZV and HSV need not use a different mechanism for axonal sorting. Like PRV, HSV-1 relies on Us9 and the gE/gI complex to sort viral structural proteins into axons of infected neurons (24, 34, 39, 44), and deletion of either HSV-1 Us9 or gE blocked anterograde, transneuronal spread in the mouse and rat visual systems (24, 34, 44). Snyder et al. also showed that deletion of gE, gI, or Us9 had a marked impact on the axonal sorting of HSV-1 capsids and glycoproteins in differentiated SK-N-SH neurons (39). Thus, HSV-1 also requires the presence of both Us9 and gE/gI for efficient anterograde sorting and spread though the relative importance of these proteins is "weighted" differently than in PRV (i.e., HSV gE/gI has a more prominent role in axonal sorting than PRV gE/gI). An important follow-up experiment will be to express HSV Us9 and gE/gI in a PRV background (with deletions of the same three genes) to examine whether complementation in anterograde spread would then occur.

Our data also suggest that HSV-1 Us9 is an integral membrane protein like the other Us9 homologs and not a tegument protein, as originally described by Frame et al. (22). Interest-

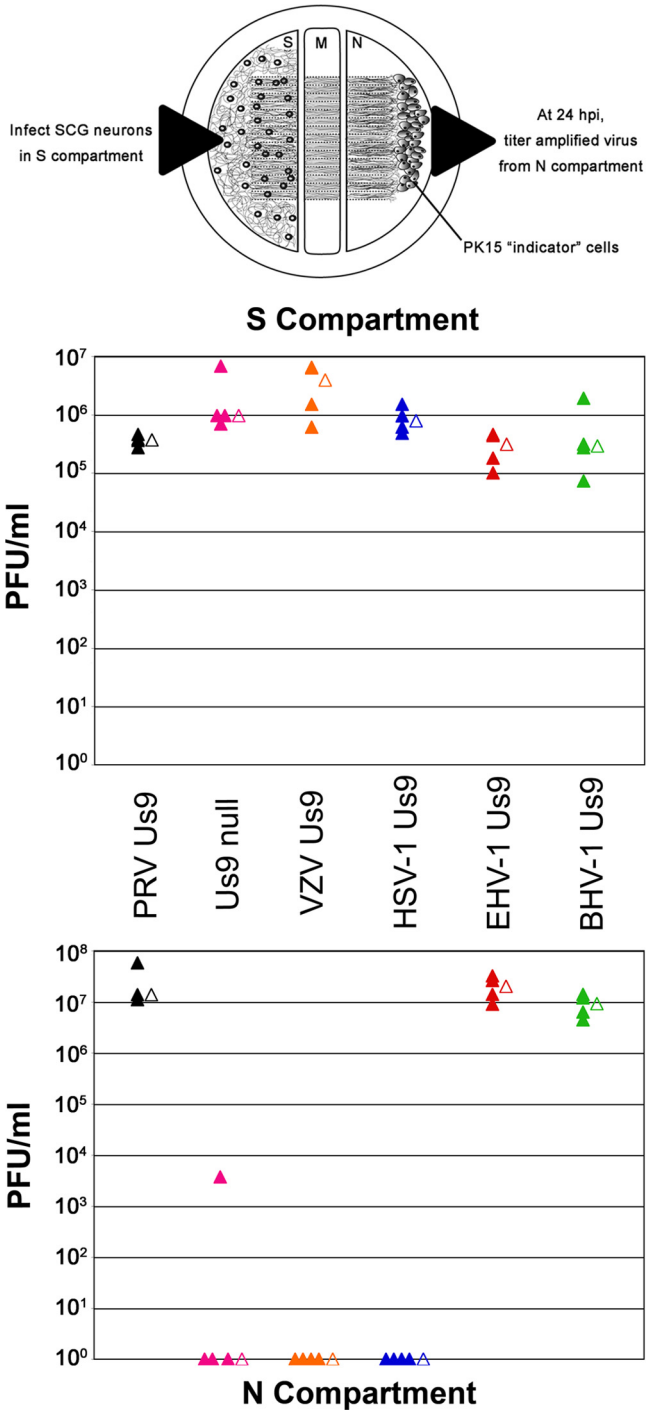

FIG. 5. Compensation for the loss of PRV Us9 in anterograde, neuron-to-cell spread of infection. A schematized representation (schematic adapted from reference 26) of the compartmented chamber system is present at the top of the figure. Cell bodies in compartment S were infected at an MOI of 10 with PRV 328 (PRV Us9; positive control), PRV 161 (Us9 null; negative control), PRV 334 (VZV Us9), PRV 335 (HSV-1 Us9), PRV 336 (EHV-1 Us9), and PRV 337 (BHV-1 Us9). Four chambers were used for each type of infection (closed symbols). At 24 hpi, medium and infected cells were harvested together from either compartment S or N (the top and bottom plots, respectively). Total PFU/ml were determined for each chamber. The mean value for the four samples is denoted by the offset open symbol.

ingly, Frame et al. noted the presence of "a large hydrophobic region at the carboxy-terminus of the molecule [HSV Us9] providing potential for association with membrane lipid." However, they ultimately concluded that HSV Us9 was a tegument protein after noting a string of arginine residues (preceding the transmembrane domain) that represented a nuclear localization signal (22). We suggest that this conserved basic region is not a nuclear localization signal but, rather, an important charged domain that establishes the topology of integral membrane proteins in the lipid bilayer (see the positive-inside rule in references 31, 33, and 43).

Frame et al. also performed immunogold electron microscopy on nuclei of infected BHK cells using Us9 antiserum (based on the idea that HSV-1 Us9 was a tegument protein that was targeted to the nucleus). They noted that few gold particles were present in their sections, perhaps due to "low abundance of the antigen and weak nature of the antipeptide serum." However, gold particles that were present seemed clustered around viral capsids (22). LaVail et al. also examined the distribution of HSV-1 Us9 in retinal ganglion cells using electron microscopy immunohistochemistry (24). They noted heavy labeling of HSV Us9 antigen on the Golgi apparatus and endoplasmic reticulum, consistent with that of a membrane protein. Interestingly, they also found Us9 signal that associated with capsids though variability in staining was noted (i.e., immunoreactive and immunonegative capsids could be observed in the same field) (24). Snyder and colleagues recently proposed that HSV-1 Us9 could be peripherally associated with membranes and also interact with nonenveloped, cytosolic capsids (39). Our findings suggest that HSV Us9 is an integral membrane protein similar to the other PRV Us9 homologs, with a type II topology, and not just peripherally associated with the lipid bilayer. As such, it is difficult to reconcile how it could also function as essentially a soluble tegument protein, directly interacting with viral capsids (24, 39) (the N-terminal domain of Us9 is too short to span the entire length of the tegument to fully bridge the viral envelope and viral capsid).

TA membrane proteins have a unique biology as they must be posttranslationally inserted into their target membrane since the hydrophobic domain emerges from the ribosome only after translation has terminated (reviewed in reference 2). It is currently believed that TA proteins can be inserted into three target membranes depending on the hydrophobicity of the transmembrane domain and flanking residues: the mitochondrial outer membrane, perixosomes, or the ER (2). Based on the observation that Us9 proteins have a steady-state accumulation in the TGN, we predict that they are posttranslationally inserted into the ER membrane and subsequently traffic through the secretory pathway to the TGN. Interestingly, Schuldiner et al. recently showed that the GET complex (consisting of Get1, Get2, and Get3) mediates the insertion of TA proteins into the ER membrane (38). Get3 recognizes the transmembrane domain of TA proteins and binds to the Get1/Get2 receptor complex for membrane insertion (38). Thus, it will be of interest to test whether these viral TA proteins, i.e., PRV Us9 and its homologs, are inserted into ER membranes via the GET complex.

Future studies will focus on the identification of viral and/or cellular proteins that interact with PRV Us9 and its homologs. The identification of these proteins and of those that interact with gE/gI will play a central role in understanding how virus

particles undergo the complex process of axonal sorting and anterograde transport.

ACKNOWLEDGMENTS

We thank Jennifer Lippincott-Schwartz (NIH), Chuck Grose (University of Iowa), D. J. O'Callaghan (Louisiana State University), S. I. Chowdhury (Louisiana State University), Jeffrey Cohen (NIH), and Harvey Friedman (University of Pennsylvania) for kindly providing reagents for this study. Alex Flood provided reagents and valuable advice for early aspects of this work. We also appreciate the input and advice from other members of the Enquist lab.

M.G.L. was supported by The American Cancer Society Eastern Division, Mercer Board Postdoctoral Fellowship (PF-08-264-01-MBC). M.P.T. and C.D.K. were supported by the National Institutes of Health (grants R01 33506 and R01 33063 to L.W.E.).

REFERENCES

1. **Ben-Porat, T., and A. S. Kaplan.** 1985. Molecular biology of pseudorabies virus, p. 105–173. *In* B. Roizman (ed.), The herpesviruses. Plenum, New York, NY.
2. **Borgese, N., S. Brambillasca, and S. Colombo.** 2007. How tails guide tail-anchored proteins to their destinations. Curr. Opin. Cell Biol. **19:**368–375.
3. **Borgese, N., S. Colombo, and E. Pedrazzini.** 2003. The tale of tail-anchored proteins: coming from the cytosol and looking for a membrane. J. Cell Biol. **161:**1013–1019.
4. **Brandimarti, R., and B. Roizman.** 1997. Us9, a stable lysine-less herpes simplex virus 1 protein, is ubiquitinated before packaging into virions and associates with proteasomes. Proc. Natl. Acad. Sci. USA **94:**13973–13978.
5. **Brideau, A. D., B. W. Banfield, and L. W. Enquist.** 1998. The Us9 gene product of pseudorabies virus, an alphaherpesvirus, is a phosphorylated, tail-anchored type II membrane protein. J. Virol. **72:**4560–4570.
6. **Brideau, A. D., J. P. Card, and L. W. Enquist.** 2000. Role of pseudorabies virus Us9, a type II membrane protein, in infection of tissue culture cells and the rat nervous system. J. Virol. **74:**834–845.
7. **Brideau, A. D., T. del Rio, E. J. Wolffe, and L. W. Enquist.** 1999. Intracellular trafficking and localization of the pseudorabies virus Us9 type II envelope protein to host and viral membranes. J. Virol. **73:**4372–4384.
8. **Brideau, A. D., M. G. Eldridge, and L. W. Enquist.** 2000. Directional transneuronal infection by pseudorabies virus is dependent on an acidic internalization motif in the Us9 cytoplasmic tail. J. Virol. **74:**4549–4561.
9. **Ch'ng, T., E. A. Flood, and L. W. Enquist.** 2005. Culturing primary and transformed neuronal cells for studying pseudorabies virus infection. Methods Mol. Biol. **292:**299–316.
10. **Ch'ng, T. H., and L. W. Enquist.** 2005. Efficient axonal localization of alphaherpesvirus structural proteins in cultured sympathetic neurons requires viral glycoprotein E. J. Virol. **79:**8835–8846.
11. **Ch'ng, T. H., and L. W. Enquist.** 2005. Neuron-to-cell spread of pseudorabies virus in a compartmented neuronal culture system. J. Virol. **79:**10875–10889.
12. **Ch'ng, T. H., P. G. Spear, F. Struyf, and L. W. Enquist.** 2007. Glycoprotein D-independent spread of pseudorabies virus infection in cultured peripheral nervous system neurons in a compartmented system. J. Virol. **81:**10742–10757.
13. **Chowdhury, S. I., S. Mahmood, J. Simon, A. Al-Mubarak, and Y. Zhou.** 2006. The Us9 gene of bovine herpesvirus 1 (BHV-1) effectively complements a Us9-null strain of BHV-5 for anterograde transport, neurovirulence, and neuroinvasiveness in a rabbit model. J. Virol. **80:**4396–4405.
14. **Chowdhury, S. I., M. Onderci, P. S. Bhattacharjee, A. Al-Mubarak, M. L. Weiss, and Y. Zhou.** 2002. Bovine herpesvirus 5 (BHV-5) Us9 is essential for BHV-5 neuropathogenesis. J. Virol. **76:**3839–3851.
15. **Clase, A. C., M. G. Lyman, T. del Rio, J. A. Randall, C. M. Calton, L. W. Enquist, and B. W. Banfield.** 2003. The pseudorabies virus Us2 protein, a virion tegument component, is prenylated in infected cells. J. Virol. **77:**12285–12298.
16. **Cohen, J. I., H. Sato, S. Srinivas, and K. Lekstrom.** 2001. Varicella-zoster virus (VZV) ORF65 virion protein is dispensable for replication in cell culture and is phosphorylated by casein kinase II, but not by the VZV protein kinases. Virology **280:**62–71.
17. **Dolan, A., F. E. Jamieson, C. Cunningham, B. C. Barnett, and D. J. McGeoch.** 1998. The genome sequence of herpes simplex virus type 2. J. Virol. **72:**2010–2021.
18. **Enquist, L. W., and J. P. Card.** 2003. Recent advances in the use of neurotropic viruses for circuit analysis. Curr. Opin. Neurobiol. **13:**603–606.
19. **Favoreel, H. W., T. C. Mettenleiter, and H. J. Nauwynck.** 2004. Copatching and lipid raft association of different viral glycoproteins expressed on the surfaces of pseudorabies virus-infected cells. J. Virol. **78:**5279–5287.
20. **Feierbach, B., M. Bisher, J. Goodhouse, and L. W. Enquist.** 2007. In vitro analysis of transneuronal spread of an alphaherpesvirus infection in peripheral nervous system neurons. J. Virol. **81:**6846–6857.
21. **Flowers, C. C., and D. J. O'Callaghan.** 1992. The equine herpesvirus type 1 (EHV-1) homolog of herpes simplex virus type 1 US9 and the nature of a major deletion within the unique short segment of the EHV-1 KyA strain genome. Virology **190:**307–315.
22. **Frame, M. C., D. J. McGeoch, F. J. Rixon, A. C. Orr, and H. S. Marsden.** 1986. The 10K virion phosphoprotein encoded by gene US9 from herpes simplex virus type 1. Virology **150:**321–332.
23. **Kanaani, J., G. Patterson, F. Schaufele, J. Lippincott-Schwartz, and S. Baekkeskov.** 2008. A palmitoylation cycle dynamically regulates partitioning of the GABA-synthesizing enzyme GAD65 between ER-Golgi and post-Golgi membranes. J. Cell Sci. **121:**437–449.
24. **LaVail, J. H., A. N. Tauscher, A. Sucher, O. Harrabi, and R. Brandimarti.** 2007. Viral regulation of the long distance axonal transport of herpes simplex virus nucleocapsid. Neuroscience **146:**974–985.
25. **Leung-Tack, P., J. C. Audonnet, and M. Riviere.** 1994. The complete DNA sequence and the genetic organization of the short unique region (US) of the bovine herpesvirus type 1 (ST strain). Virology **199:**409–421.
26. **Lyman, M. G., D. Curanovic, A. D. Brideau, and L. W. Enquist.** 2008. Fusion of enhanced green fluorescent protein to the pseudorabies virus axonal sorting protein Us9 blocks anterograde spread of infection in mammalian neurons. J. Virol. **82:**10308–10311.
27. **Lyman, M. G., D. Curanovic, and L. W. Enquist.** 2008. Targeting of pseudorabies virus structural proteins to axons requires association of the viral Us9 protein with lipid rafts. PLoS Pathog **4:**e1000065.
28. **Lyman, M. G., B. Feierbach, D. Curanovic, M. Bisher, and L. W. Enquist.** 2007. Pseudorabies virus Us9 directs axonal sorting of viral capsids. J. Virol. **81:**11363–11371.
29. **McGeoch, D. J., and S. Cook.** 1994. Molecular phylogeny of the Alphaherpesvirinae subfamily and a proposed evolutionary timescale. J. Mol. Biol. **238:**9–22.
30. **Mettenleiter, T. C.** 2000. Aujeszky's disease (pseudorabies) virus: the virus and molecular pathogenesis—state of the art, June 1999. Vet. Res. **31:**99–115.
31. **Parks, G. D., and R. A. Lamb.** 1993. Role of NH2-terminal positively charged residues in establishing membrane protein topology. J. Biol. Chem. **268:**19101–19109.
32. **Patterson, G. H., K. Hirschberg, R. S. Polishchuk, D. Gerlich, R. D. Phair, and J. Lippincott-Schwartz.** 2008. Transport through the Golgi apparatus by rapid partitioning within a two-phase membrane system. Cell **133:**1055–1067.
33. **Persson, B., and P. Argos.** 1996. Topology prediction of membrane proteins. Protein Sci. **5:**363–371.
34. **Polcicova, K., P. S. Biswas, K. Banerjee, T. W. Wisner, B. T. Rouse, and D. C. Johnson.** 2005. Herpes keratitis in the absence of anterograde transport of virus from sensory ganglia to the cornea. Proc. Natl. Acad. Sci. USA **102:**11462–11467.
35. **Pomeranz, L. E., A. E. Reynolds, and C. J. Hengartner.** 2005. Molecular biology of pseudorabies virus: impact on neurovirology and veterinary medicine. Microbiol. Mol. Biol. Rev. **69:**462–500.
36. **Roizman, B., and D. M. Knipe.** 2001. Herpes simplex viruses and their replication, p. 2399–2459. *In* D. M. Knipe, P. M. Howley, D. E. Griffin, R. A. Lamb, M. A. Martin, B. Roizman, and S. E. Straus (ed.), Fields virology, 4th ed. Lippincott Williams & Wilkins, Philadelphia, PA.
37. **Roizman, B., and P. E. Pellet.** 2001. The Family *Herpesviridae:* a brief introduction. *In* D. M. Knipe, P. M. Howley, D. E. Griffin, R. A. Lamb, M. A. Martin, B. Roizman, and S. E. Straus (ed.), Fields virology, 4th ed. Lippincott Williams & Wilkins, Philadelphia, PA.
38. **Schuldiner, M., J. Metz, V. Schmid, V. Denic, M. Rakwalska, H. D. Schmitt, B. Schwappach, and J. S. Weissman.** 2008. The GET complex mediates insertion of tail-anchored proteins into the ER membrane. Cell **134:**634–645.
39. **Snyder, A., K. Polcicova, and D. C. Johnson.** 2008. Herpes simplex virus gE/gI and US9 proteins promote transport of both capsids and virion glycoproteins in neuronal axons. J. Virol. **82:**10613–10624.
40. **Telford, E. A., M. S. Watson, K. McBride, and A. J. Davison.** 1992. The DNA sequence of equine herpesvirus-1. Virology **189:**304–316.
41. **Telford, E. A., M. S. Watson, J. Perry, A. A. Cullinane, and A. J. Davison.** 1998. The DNA sequence of equine herpesvirus-4. J. Gen. Virol. **79:**1197–1203.
42. **Tomishima, M. J., and L. W. Enquist.** 2001. A conserved alpha-herpesvirus protein necessary for axonal localization of viral membrane proteins. J. Cell Biol. **154:**741–752.
43. **von Heijne, G., and Y. Gavel.** 1988. Topogenic signals in integral membrane proteins. Eur. J. Biochem. **174:**671–678.
44. **Wang, F., W. Tang, H. M. McGraw, J. Bennett, L. W. Enquist, and H. M. Friedman.** 2005. Herpes simplex virus type 1 glycoprotein e is required for axonal localization of capsid, tegument, and membrane glycoproteins. J. Virol. **79:**13362–13372.
45. **Whealy, M. E., J. P. Card, A. K. Robbins, J. R. Dubin, H. J. Rziha, and L. W. Enquist.** 1993. Specific pseudorabies virus infection of the rat visual system requires both gI and gp63 glycoproteins. J. Virol. **67:**3786–3797.
46. **Whitley, R. J., and M. Schlitt.** 1991. Encephalitis caused by herpesviruses, including B virus, p. 41–86. *In* R. J. Whitely, M. J. Scheld, and D. T. Durack (ed.), Infections of the central nervous system. Raven Press, New York.
47. **Wittmann, G. a. H. J. R.** 1989. Herpesvirus diseases of cattle, horses and pigs. Kluwer Academic Publishers, Dordrecht, The Netherlands.